

Physics

Electricity & Magnetism fields

Okayama University

Year 1990

3-D magnetic field analysis using special
elements

Takayoshi Nakata
Okayama University

K. Fujiwara
Okayama University

N. Takahashi
Okayama University

Y. Shiraki
Okayama University

This paper is posted at eScholarship@OUDIR : Okayama University Digital Information Repository.

http://escholarship.lib.okayama-u.ac.jp/electricity_and_magnetism/24

3-D MAGNETIC FIELD ANALYSIS USING SPECIAL ELEMENTS

T. Nakata, N. Takahashi, K. Fujiwara and Y. Shiraki

Dept. of Electrical Engineering, Okayama Univ.,
Okayama 700, Japan

ABSTRACT

3-D special elements called the "gap element", the "expanding element" and the "shielding element" have been conceived for discretizing narrow gaps in an iron core, the long legs of a transformer core and the thin shielding plates. The concept of the 3-D special element and its finite element formulation are described. The special elements are applied to a few models and the effects of these elements on accuracy and CPU time are discussed. It is shown that CPU time can be reduced by using the special elements.

1. INTRODUCTION

We have already developed the "gap element[1,2]", which has energy but no area, for 2-D magnetic field analysis. As this element has no area, it is very easy to put new gaps into desired positions in the mesh, to remove them or to modify the gap lengths freely. Moreover, the "expanding element[3]" and "shielding element[3]" have also been developed for analyzing 2-D magnetic fields in a transformer core and 2-D eddy currents in a thin conducting plate respectively.

In this paper, these special elements are expanded to the case of 3-D magnetic field analysis using the A- ϕ method[4].

2. SPECIAL ELEMENTS

When the gap length D in a magnetic core is very short, it can be assumed that the flux is perpendicular to the gap between high permeability materials as shown in Fig.1(a). Such a region V_s can be subdivided by, for example, 2-D quadrilateral elements as shown in Fig.1(d) instead of conventional 3-D elements such as hexahedral elements. The leg of the transformer core of which the length D is long and the flux is parallel to the leg (Fig.1(b)), and the conducting plate of which the thickness D is small (Fig.1(c)) can also be represented by quadrilateral elements (Fig.1(d)). Such additional 2-D elements are referred to as the "gap element", the "expanding element" and the "shielding element" respectively. The "special element" is a general name for these elements. The special element has no volume, but has nearly the same energy as the gap, leg and conducting plate shown in Figs.1(a), (b) and (c).

The special element has the following advantages:

- As the special element has no volume, it is easy to put new gaps, legs or conducting plates in desired positions in the mesh or to remove them.
- As the modification of the length D is also easy, the influence of D on the magnetic characteristics can be examined easily by using the special element.
- When the special element is used, the ill-conditioning of the coefficient matrix due to narrow gaps and thin conducting plates can be avoided. Therefore, the CPU time using the special element can be reduced when compared with that using the flat conventional element, because the number of iterations of the ICCG method[5] is decreased.

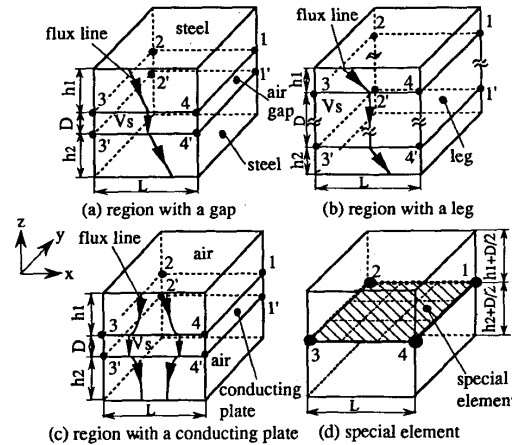


Fig. 1 Idea of various 3-D special elements.

3. DISTRIBUTIONS OF POTENTIALS IN SPECIAL ELEMENTS

The x - and y -components of the flux density B are given by the following equations[6]:

$$B_x = \partial A_z / \partial y - \partial A_y / \partial z \quad (1)$$

$$B_y = \partial A_x / \partial z - \partial A_z / \partial x \quad (2)$$

where A_x , A_y and A_z are the x -, y - and z -components of the magnetic vector potential A .

As the vector potential A in the regions V_s shown in Figs.1(a) to (c) is constant in the z -direction, the following equation can be obtained:

$$\partial A / \partial z = 0 \quad (3)$$

As the x - and y -components B_x and B_y are both equal to zero, the following equation can be obtained from Eqs.(1) to (3):

$$\partial A_z / \partial x = \partial A_z / \partial y = 0 \quad (4)$$

From Eqs.(3) and (4), A_z is constant in the region V_s . Thus, A_z is assumed to be zero as follows:

$$A_z = 0 \quad (5)$$

As the shielding element is to be used in the eddy current analysis, the distribution of the electric scalar potential ϕ as well as the vector potential A should be investigated. The z -component J_{ez} of the eddy current density J_e can be given by [6]

$$J_{ez} = -\sigma (\partial A_z / \partial t + \partial \phi / \partial z) \quad (6)$$

where σ is the conductivity. As the shielding plate is very thin, the scalar potential ϕ can be assumed to be constant in the z -direction as follows:

$$\partial \phi / \partial z = 0 \quad (7)$$

From Eqs.(3) and (7), the following relationships between each component of the vector potential A and the scalar potential ϕ at the nodes 1 to 4 and 1' to 4' in Figs.1(a) to (c) can be assumed:

$$A_{ij} = A_{ij}', \quad \phi_j = \phi_j'$$

$$(i=x,y,z, \quad j=1, \dots, 4, \quad j'=1', \dots, 4') \quad (8)$$

Equations (5) and (8) eliminate the vector potentials $A_{xj}, A_{xj'}, A_{yj}, A_{yj'}$ and the scalar potential ϕ_j' from the unknowns.

4. FINITE ELEMENT FORMULATION

3-D magnetic fields with eddy currents are governed by the following equations[4]:

$$\text{rot}(\nu \text{rot} \mathbf{A}) = \mathbf{J}_0 - \sigma \left(\frac{\partial \mathbf{A}}{\partial t} + \text{grad} \phi \right) \quad (9)$$

$$\text{div} \left\{ -\sigma \left(\frac{\partial \mathbf{A}}{\partial t} + \text{grad} \phi \right) \right\} = 0 \quad (10)$$

where \mathbf{J}_0 is the magnetizing current density and ν is the reluctivity. The following equations can be obtained by Galerkin's method from Eqs.(9) and (10)[4].

$$G_{0i} = - \iiint_V (\text{grad} N_i) \times (\nu \text{rot} \mathbf{A}) dV + \iiint_{V_c} N_i \mathbf{J}_0 dV + \iiint_{V_e} N_i \sigma \left(\frac{\partial \mathbf{A}}{\partial t} + \text{grad} \phi \right) dV \quad (11)$$

$$G_{ei} = \iiint_{V_e} \sigma \text{grad} N_i \cdot \left(\frac{\partial \mathbf{A}}{\partial t} + \text{grad} \phi \right) dV \quad (12)$$

where N_i is the interpolation function[6] and V is the analyzed region. Subscripts c and e show the regions of the windings and the conductors with eddy currents, respectively. Assuming that the potentials are constant along the flux line as shown in Eq.(8), the weighted residuals G_{0i} and G_{ei} of Galerkin's method for the special elements are given by

$$G_{0i} = -D \iint_{S_s} (\text{grad} N_i) \times (\nu \text{rot} \mathbf{A}) dS + D \iint_{S_{se}} N_i \sigma \left(\frac{\partial \mathbf{A}}{\partial t} + \text{grad} \phi \right) dS \quad (13)$$

$$G_{ei} = D \iint_{S_{se}} \sigma \text{grad} N_i \cdot \left(\frac{\partial \mathbf{A}}{\partial t} + \text{grad} \phi \right) dS \quad (14)$$

where S_s is the region where the gap and the expanding elements are defined. In the case of the gap element, the reluctivity ν is changed to ν_0 (the reluctivity of air). S_{se} is for the shielding element. As the magnetizing current does not flow in the special element, \mathbf{J}_0 is removed from Eq.(13). Equations (13) and (14) show that 3-D problem can be reduced to 2-D problem by applying the special element. If the length D is replaced by 1, Eqs.(13) and (14) represent the equations for an ordinary 2-D element. The gaps, legs and shielding plates can easily be discretized by adding Eqs.(13) and (14) to the usual linear equations for the 3-D finite element method.

When the gap element is applied, both nodes 1,2,3,4 and 1',2',3',4' are moved symmetrically to the center line between them as shown in Fig.1(d). Therefore the length of the iron part has to be increased by D . The energy of the increased iron part, however, can be neglected because the permeability of the iron part is very high compared with that of the gap part and the gap length D is short.

5. EXAMPLES OF APPLICATION

In order to verify the usefulness of the special elements, a few analyses are carried out. In the region where the special element is not applied, the ordinary 1st-order brick element is used.

5.1 Gap element

The accuracy of the gap element is investigated by using the model with a gap as shown in Fig.2. The

current in the winding is dc. The 3-D magnetic field is analyzed neglecting saturation. As the model is symmetric, only 1/4 region ($-40 < x < 140$, $0 < y < 60$, $0 < z < 120$ mm) need be analyzed. The number of elements, etc. are shown in Table 1.

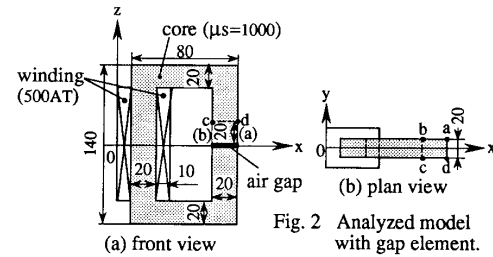


Fig. 2 Analyzed model with gap element.

Table 1 Discretization data and CPU time

item		using gap element	using ordinary element
number of elements	except gap region	4928	5150
	gap region	150	450
number of nodes		6072	6864
CPU time (s)	ICCG	299	1445
	total	332	1482

computer used : NEC supercomputer SX-1E
(maximum speed: 285MFLOPS)

Figure 3 shows the effect of the gap length D on the error ϵ_B in the flux density. ϵ_B is defined by

$$\epsilon_B = \frac{B_g - B_0}{B_0} \times 100 (\%) \quad (15)$$

where B_g is the average flux density on the plane a-b-c-d-a in Fig.2 calculated using the gap element. B_0 is calculated using a conventional mesh subdivided into brick elements. L is the width of the gap (=20mm). If the permissible error is less than 1%, the gap element can be used in practice under the condition that the ratio D/L is smaller than about 0.04, as shown in Fig.3.

Figure 4 shows the comparison of the CPU time. The CPU time is not affected by the gap length D when the gap element is used. The CPU time using only conventional elements is very much increased as D is decreased because the coefficient matrix becomes ill-conditioned as D decreases.

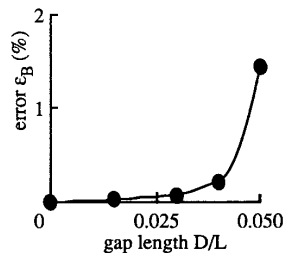


Fig. 3 Effect of gap length on the error of flux density.

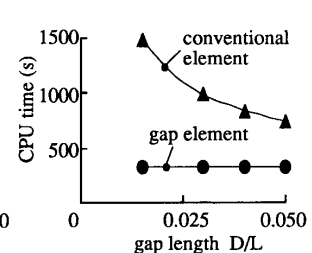


Fig.4 CPU time.

5.2 Shielding element

The effects of an aluminum shield on flux and eddy current distributions are investigated using the model shown in Fig.5. The fields are produced by the exciting current at 50 and 200 Hz. The ampere turns of

the coil are set to 3000AT(peak value). The conductivities of aluminum and steel are 3.56×10^7 and 7.51×10^6 S/m respectively, and the relative permeability of the steel is assumed to be 1000. A quarter model ($0 < x < 500$, $0 < y < 500$, $-150 < z < 500$ mm) is analyzed. The number of elements, etc. are shown in Table 2. The CPU time using the shielding element is reduced compared with that using only conventional brick elements. This tendency is similar to the case of the gap element.

Figure 6 shows the comparison of the z-component B_z of the flux density along the line a-b ($y=12.5$, $z=10$ mm) shown in Fig.5. The thickness D of the plate is equal to 1mm. The flux density is measured using a small search coil (diameter:3mm, height:0.6mm, 20turns). The effect of the shielding plate on the flux density at 200Hz is more remarkable than at 50Hz.

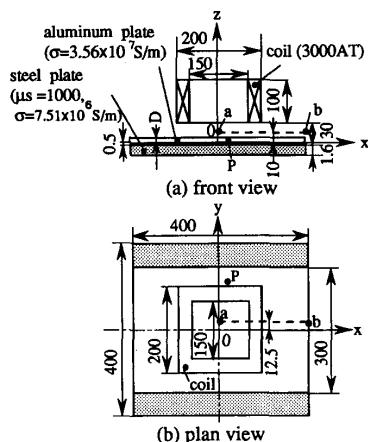


Fig. 5 Analyzed model with shielding element.

Table 2 Discretization data and CPU time

item		using shielding element	using ordinary element
number of elements	except conducting region	2057	2115
	conducting region	63	63
number of nodes		2592	2736
CPU time (s)	ICCG	805	1142
	total	821	1161

computer used : NEC supercomputer SX-1E
(maximum speed : 285 MFLOPS)

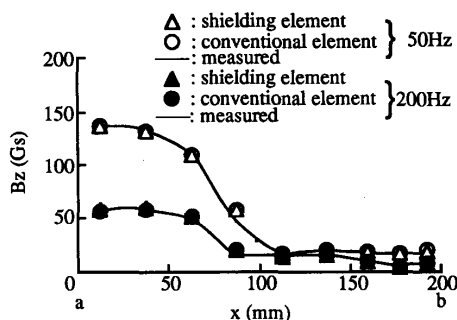


Fig. 6 Distributions of B_z ($D=1$ mm).

Figure 7 shows the effect of the thickness D of the shielding plate on the error ϵ_j of the eddy current density. δ is the skin depth. The definition of the error ϵ_j is the same as Eq.(15). The eddy current density is examined at the point P ($x=12.5$, $y=110$, $z=1$ mm) in the shielding plate. If the permissible error is less than 1%, the shielding element can be used when $D/\delta < 0.11$.

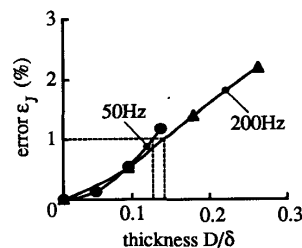


Fig. 7 Effects of thickness of the shielding plate on the error of eddy current density ($x=12.5$, $y=110$, $z=1$ mm).

6. CONCLUSIONS

The results obtained can be summarized as follows:

- (1) The program taking into account the 3-D special elements can be easily modified by adding 2-D equations to the ordinary 3-D code.
- (2) The CPU time can be reduced to about 2/3 of that needed for the case of using only conventional elements.
- (3) The range of application of special elements is examined from the standpoint of accuracy.

It is hoped that the application of 3-D special elements will be expanded. The expansion of the technique described in this paper to edge elements will be reported in another paper.

ACKNOWLEDGEMENT

This work was partly supported by the Grant-in-Aid for Co-operative Research (A) from the Ministry of Education, Science and Culture in Japan (No.01302031).

REFERENCES

- [1] T.Nakata, Y.Ishihara and N.Takahashi : "Finite Element Analysis of Magnetic Fields by Using Gap Element", Proceedings of Compumag Conference, Grenoble, 5.7 (1978).
- [2] T.Nakata, Y.Ishihara and N.Takahashi: "Some Useful Techniques on Implementing the Finite Element Method for Computation of Electromagnetic Fields in Electrical Machinery", Interdisciplinary Finite Element Analysis (book, Edited by J.F.Abel et al.), 545 (1981) Cornell University.
- [3] T.Nakata, N.Takahashi, Y.Kawase, T.Masuyama and K.Fujiwara: "Development of Special Elements for Magnetic Field Analysis", Papers of Technical Meeting on Rotating Machines and Static Apparatus, IEE of Japan, RM-81-37, SA-81-27 (1981).
- [4] M.V.K.Chari, A.Konrad, M.A.Palmo and J.D'Angelo : "Three-Dimensional Vector Potential Analysis for Machine Field Problems", IEEE Trans. Magnetics, MAG-18, 2, 436(1982).
- [5] J.A.Meijerink and H.A.van der Vorst : "An Iterative Solution Method for Linear Systems of Which the Coefficient Matrix is a Symmetric M-Matrix", Math. Comp., 31, 137, 148 (1977).
- [6] T.Nakata and N.Takahashi : "Finite Element Method in Electrical Engineering (the 2nd Edition)" (1988) Morikita Publishing Co., Tokyo.